Experimental Implementation Controlled SPWM Inverter based Harmony Search Algorithm

Mushtaq Najeeb*‡, Muhamad Mansor**, Ramdan Razali***, Hamdan Daniyal***, Jabbar A. F. Yahaya**

*Faculty of Electrical and Electronics Engineering, Universiti Malaysia Pahang, Pekan, Pahang, Malaysia

*Electrical Engineering Department, College of Engineering, University of Anbar, Ramadi, Iraq

**Department of Electrical Power Engineering, Universiti Tenaga Nasional, Selangor, Malaysia

*** Faculty of Electrical and Electronics Engineering, Universiti Malaysia Pahang, Pekan, Pahang, Malaysia

‡ Corresponding Author; Mushtaq Najeeb, Universiti Malaysia Pahang, Malaysia, H/P: +60182570142, eng.mushtaq2004@gmail.com

Received: 20.12.2016 Accepted: 27.02.2017

Abstract- An optimum PI controller using harmony search optimization algorithm (HS) is utilized in this research for the single-phase bipolar SPWM inverter. The aim of this algorithm is to avoid the conventional trial and error procedure which is usually applied in finding the PI coefficients in order to obtain the desired performance. Then, the control algorithm of the inverter prototype is experimentally implemented using the eZdsp F28355 board along with the bipolar sinusoidal pulse width modulation (SPWM) to control the output voltage drop under different load conditions. The proposed overall inverter design and the control algorithm are modelled using MATLAB environment (Simulink/m-file Code). The mean absolute error (MAE) formula is used as an objective function with the HS algorithm in finding the adaptive values of k_p and k_i parameters to minimize the error of the inverter output voltage. Based on the output results, the proposed voltage controller using HS algorithm based PI (HS-PI) showed that the inverter output performance is improved in terms of voltage amplitude, robustness, and convergence rate speed as compared to PSO algorithm based PI (PSO-PI). This is to say that the proposed controller provides a good dynamic responses in both cases; transient and steady-state. Finally, the experimental setup result of the inverter controller is verified to validate the simulation results.

Keywords Harmony search algorithm (HS), eZdsp F28335 board, mean absolute error (MAE), C code for the sine PWM, and transient response.

1. Introduction

The topic of alternative energy sources is one of the most active research area today for energy demand generation. Photovoltaic solar energy (PV) is one of the important energy sources especially for the applications of rural locations [1-7]. This is because it has some advantages such as environment friendly, mentanice free, and it has long life span as compared to the traditional energy sources like fossil fuel [8-10]. A PV source is only supplying a dc voltage, therefore, an inverter device is required to convert a DC to an AC source because of the most PV inverter applications are connected to the AC loads [11-15]. So, the main important feature of the inverter design is the controller improvement. Secondly, the controller ability is to provide a non-voltage drop in the output waveform and keep a constant frequency regardless of different loads are externally connected [16,17].

Thus, the successful application of the PV inverter system depends on the effectiveness strategy of the controller algorithm especially along with the digital signal processing boards' developments in the last decades. Therefore, there are a lot of various control algorithms have been carried out in the literature to solve the voltage control problems. The author in [18] has implemented a PI controller with a PWM algorithm for the PV inverter system using eZdsp F2812 board to keep the voltage waveform as a sinusoidal. Similarly, the researchers in [19] have also proposed a conventional controller of proportional-integral design to control the boost converter for the inverter system in order to get a good performance. In a related research, a field programmable gate array (FPGA) has been used in the PV inverter systems to develop the control algorithm described in [20, 21] but it considered a time consuming task because it needs a wide knowledge in software programming. For a real

time hardware setup, the reference [22] has used the platform of dSPACE DS1104 control unit to implement the PI controller of three-phase PV inverter system for a good dynamic performance. Also, same control unit has been used in [23] to enable the user to develop the control algorithm by employing the available features of Matlab/Simulink tools with the library blocksets in order to link the simulated model directly into the dSPACE controller. Another application approach of dSPACE real-time data acquisition unit has been integrated in the grid-connected system by [24], fuzzy logic controller was implemented to regulate the inverter output voltage. However, the method of PI parameters tuning is very essential for the good control algorithm. Therefore, many optimization techniques of artificial intelligence have been used in the PV inverters to achieve the desired performance. For example, an optimal strategy of PI controller with a DC voltage regulation source was suggested in [25] for the photovoltaic grid-connected. A particle swarm optimization algorithm (PSO) has been applied for different applications to optimize the settings of the PI parameters under small disturbances of load conditions [26-30]. In addition, an optimal PI controller has been proposed in [31] utilizing genetic algorithm (GA) to control the photovoltaic system performance especially the output voltage. Yet, a tuning method for finding PI coefficients using harmony search optimization algorithm has not been applied in the SPWM inverter applications.

In this research, the harmony search optimization algorithm (HS) based PI approach is utilized to enhance the controller performance of the single-phase bipolar SPWM inverter. The aim of this algorithm is to avoid the conventional trial and error method in finding the PI coefficients (k_p ,k_i), then these coefficients have been used to evaluate the controller effectiveness by minimizing the mean absolute error (MAE) of the output voltage. The inverter system and the control algorithm are modelled using the environment of MATLAB (Simulink/Code). After that, the control algorithm of the inverter prototype is experimentally implemented in the eZdsp F28335 board to validate the proposed controller performance under different load conditions. An explanation of other details is discussed in the following sections, section 2 describes the overall inverter system design. Section 3 describes the inverter model using a conventional PI approach. Section 4 explains the proposed optimum voltage controller which includes an overview of HS algorithm and the optimal procedure how to obtain the PI parameters. The implementation of the control algorithm and the experimental setup of the proposed inverter system are presented in section 5 and 6 respectively. Eventually, the discussion of experimental and simulation results are presented in section 7.

2. Overall Inverter Description

Fig. 1 shows the overall inverter considered in this research, which includes both power and control stages. The power stage consists of a DC voltage source (V_{dc}), full bridge configuration with four switches (IGBTs) which can be modulated using the bipolar SPWM method followed by an appropriate LC filter circuit which filters out the frequency switching f_s of the bridge circuit as well as improve the voltage waveform linked to the load, and two different loads; resistive and inductive. Regarding the control stage; it consists of a computer, DSP board, and the get driver circuit. The output voltage of the inverter (V_{Load}) can be sensed at the terminal of two different loads (R, RL) by using a voltage feedback sensor and it can be represented as [32]:

$$V_{load} = V \sin \omega t \quad (1)$$

Where V is the peak voltage and ω is the fundamental frequency of the inverter output. However, the generated error between the reference and the measured voltages is then sent to the proposed controller which includes the harmony search algorithm based PI approach. Next, a comparison between $V_{control}$ and $V_{carrier}$ based bipolar SPWM method is done to derive the inverter by generating $S_1$and S_2 signals in order to obtain the desired output. All these steps are implemented using the TMS320F28335 board, which is a popular platform to be used based on the inverter topology required. In general, the differential equations which describe the behavior of the inverter system in time domain are presented below [33]:

$$L \frac{d_{I_L}}{d_t} = mV_{dc} - V_{Load} \quad (2)$$

$$C \frac{d_{V_{Load}}}{d_t} = I_C = I_L - I_{Load} \quad (3)$$

Where m is the control switching variable, it can take either 1 if the switch S_1 is on or -1 if the switch S_2 is on, and mV_{dc} is the inverter output voltage ($V_{inv\ out}$).

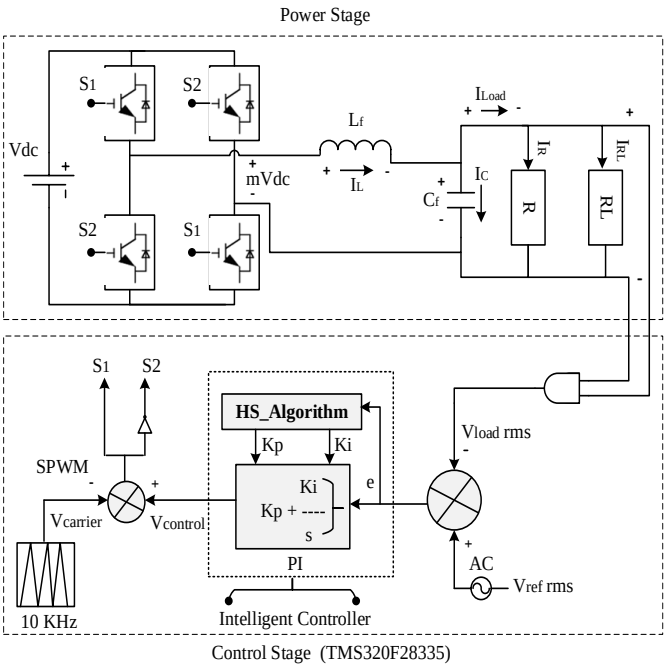

Fig.1. Overall Inverter

According to [34], the typical transfer function of the classical PI controller in terms of Laplace domain is described below:

$$G_{PI}(s) = \frac{U(s)}{E(s)} = K_p + \frac{K_i}{s} \quad (4)$$

Where, K_p is the proportional gain, K_i is the integration gain, U(s) and E(s) are the control and the error signals.

In fig. 1, the input of the PI controller is the error (e) signal and the output is the voltage control ($V_{control}$). Thus, the voltage control $V_{control}$ equation which describes the PI controller in time domain is illustrated below in equation (5). On the other hand, the designer must adjust the boundary values of the PI coefficients (k_p, k_i) in any standard design by using trial-and-error procedure until the result is satisfied. This is considered a time consuming task. Therefore, the optimization algorithms represent the optimal and the efficient solution to find the PI coefficients [35, 36] by considering the error (e) signal is the optimization problem.

$$V_{control}(t) = k_p\, e(t) + k_i \int_0^t e(t)dt \quad (5)$$

3. Proposed Optimum PI Voltage Controller

As mentioned in the previous section that the main drawback of the conventional PI controller is the trial and error procedure to adjust the values of K_p and K_i coefficients in order to avoid the bad performance. So, this research proposes an optimum PI voltage controller using harmony search (HS) algorithm to optimize K_p and K_i coefficients to control the output voltage drop and keep the system is at a desired performance with a fast dynamic response. The HS algorithm has been widely utilized in different studies to solve a lot of optimization problems related to the applications of engineering felids such as design of steel structure, heat exchanger design, robotics, telecommunications, and so on [37] but it has not been used to solve the voltage control problems for the inverter applications under different load conditions.

3.1. HS Algorithm Overview

Harmony search (HS) is a well-known meta-heuristic optimization algorithm inspired by the modern natural phenomena, which was proposed by [38]. The basic process of this algorithm is to produce music tunes through pitching the musical instruments in order to search for a harmony. For the harmony improvisation, musicians try various musical combinations stored in their memory to get an excellent quality. Meanwhile, it is similar to the optimization process by creating a new solution using an objective function in order to improve the quality of the generated solutions and the more details can be seen in [39, 40]. In brief, the optimization process of the harmony search algorithm is shown in fig. 2 which can be concluded in five steps.

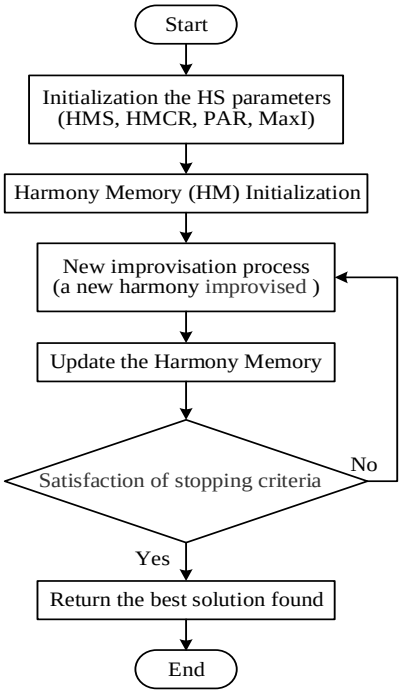

Fig. 2. Harmony search algorithm flowchart

3.2. HS Procedure to obtain the Optimal PI Parameters

In any optimization algorithm, the input vector formula to find the optimal solutions can be defined as [41];

$$\text{Min. or Max.} = Z(k), k_n \in \mathbf{K_n};\ (n = 1,2,\ldots\ldots M) \quad (6)$$

Where the input vector to the optimization algorithm is $Z(k)$, k_n is the decision parameter, $\boldsymbol{K_n}$ is the lower and upper values of each decision parameter ($L_{k_n} < \boldsymbol{K_n} < U_{k_n}$), and M is the total number of decision parameters.

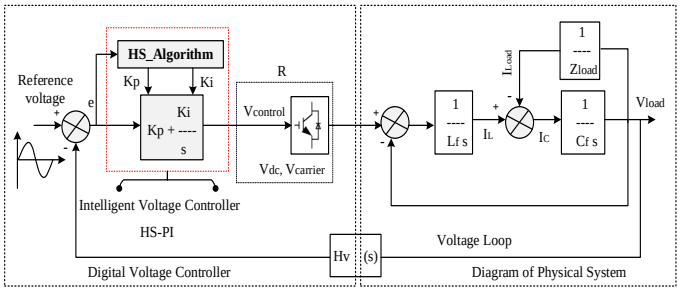

Fig. 3. Closed loop diagram of inverter model with harmony search algorithm

Based on equation (6), two decision parameters (k_p,k_i) of the input vector $Z(k)$ are used in this research to provide the optimal solutions from the HS optimization algorithm as shown in fig. 3. In addition, an objective function is required to evaluate the performance of the input vector $Z(k)$. Therefore, the mean absolute error (MAE) shown below is applied as an optimization problem at each sampling time [42].

$$\text{MAE (Min.)} = \frac{1}{L}\sum_{p=1}^{L}|e| = \frac{1}{L}\sum_{p=1}^{L}|V_{ref\,rms} - V_{Load\,rms}| \quad (7)$$

Where $V_{Load\,rms}$ is the measured feedback voltage, $V_{ref\,rms}$ is the reference voltage, and L is the number of samples used in this research.

A more explanation of the optimization process shown in fig. 2 for the harmony search algorithm based PI controller is presented as follows:

- **Parameters Initialization of HS algorithm;** the harmony memory size (HMS) is 20 or it is called the number of solution vectors, the harmony memory considering rate (HMCR) is 0.9, the pitch adjusting rate (PAR) is 0.3, and the maximum number of improvisation (MaxI) is 100.
- **Harmony memory (HM) initialization;** a matrix of (k_p,k_i) solutions is created as shown in equation (8) which is equal to the size of harmony memory (HMS). These solutions are generated randomly using the formula shown in equation (9). Then, the fitness value $f(k)$ for each row of the solution vector is calculated in the second part of equation (8) as well.

$$HM = \left\{ \begin{array}{cc|c} k_p^1 & k_i^1 & f(k^1) \\ \vdots & \vdots & \vdots \\ k_p^{HMS} & k_i^{HMS} & f(k^{HMS}) \end{array} \right\} \quad (8)$$

$$HM(k_{p,i}) = rand * (upper - lower) + lower \quad (9)$$

- **New improvisation process;** an empty solution vector of $k' = [\,]$ is generated based on the values of HMS, HMCR, and PAR. Next, a random number r_1 is generated with a range is between [0, 1]. If the HMCR is bigger than r_1, choose a decision parameter from the HM (for example, $[k_p^1 \;\ldots\; k_p^{HMS}\; or\; k_i^1 \;\ldots\; k_i^{HMS}]$) and add to the solution vector k' (means the probability of HMCR is considered). Otherwise, a new random decision parameter is generated and added to the solution vector $k' = rand * [(upper - lower) + lower]$ (means the probability of [1-HMCR] is considered) which can be increased the probability of the solutions diversity to explore the optimal values. Furthermore, the decision parameter which has been selected from HM and added to the solution vector k' will be adjusted with the PAR probability for more optimal improvement. Therefore, a second random number r_2 is generated with a range is between [0, 1]. If the PAR is bigger than r_2, add a random number to the selected decision parameter $k'_{new} = (k'_{\text{selected}} + rand)$ in order to obtain the new decision parameter (means the probability of PAR is considered). This process will stop when the size of the new decision parameter is equal to the largest solution vector in the harmony memory (HM).
- **Harmony memory (HM) Update;** if the fitness value $f(k')$ of the new solution vector k' which is generated from the improvisation process is better than the worst fitness value of the solution vector stored in the harmony memory (HM), then the new solution vector will be replaced by the old one and added to the HM. Else, the process will re-evaluate the objective function shown in equation (7) through the next iteration.
- **Stopping criteria satisfaction;** the stopping criteria of the harmony search optimization process is tested in this step. If the maximum number of the iterations (MaxI) is reached, then this process will stop and return back the best solution found ($latest\; k_p$,k_i) in the harmony memory (HM). Otherwise, step 3 and 4 are repeated.

4. Implementation of Optimal PI Controller using eZdsp F28335 Board

In recent decades, Texas Instrument TMS320F28335 is becoming very essential board for the high switching algorithms in different control applications of renewable energy sources especially the PV inverters. Therefore, the implementation of the Optimal PI Controller for the proposed hardware inverter using eZdsp F28335 board is described here to show the controller performance in the real time world under different load conditions. This section is divided into two parts, the first one gives an overview about the eZdsp F28335 unit. And, the second one explains the implementation of the proposed control algorithm.

4.1. eZdsp F28335Unit

In the real-time world, it is not easy to design and implement the control algorithms for the inverter applications using analog controllers. This is because of the analog controller depends on the large number of separated components which makes the design's cost is high especially when there is any required changes in the hardware model. Therefore, the digital signal processor such as the C2000 family of eZdsp TMS320F2833x has the ability to link the hardware of the inverter prototype by the computer (Matlab/Simulink) which can be reduced the components number and provides a higher reliability. In this research, the Harvard architecture of eZdsp TMS320F28335 board is used due to its features as compared with the previous models like TMS320F2812 board [43]. These features are as follows; operating speed is 150 MHz with a high performance, RAM chip is 68K bytes, flash memory chip is 512K bytes, single random access memory (SRAM) chip is 256K bytes, and analog to digital chip is 12-bit with 16 input channels. In addition, the F28335 board provides extra functions like general-purpose input/output (GPIO) multiplexer, CPU-timers, and control peripherals. The most important functions of the control peripherals are event manager (EVM) module which controls the switching signals and analog digital converter (ADC) which includes two sample and hold units for the sampling process. The EVM consists of general purpose timers, full compare/PWM units, capture inputs

(CAP), and quadrature encoder pulse (QEP) circuits. In the eZdsp F28335 board, the ADC receives the measured feedback signal (analog) through a sensor device and convert it to the digital signal in order to generate the system output. Furthermore, the environment of Code Composer Studio (CCS) software is used to implement the proposed control algorithm code for the sine pulse width modulation (SPWM) of the proposed inverter and monitor the overall system performance as well.

4.2. Proposed Control Algorithm

The proposed control algorithm for the closed loop diagram of the inverter system design which described in section 4 is implemented using eZdsp F28335 board. In this algorithm, the feedback voltage is initially measured using a voltage sensor which called LEM LV25-P (716029). This sensor decreases the value of the measured voltage to eZdspF28335 board's range which is from 0 to 3 volt and then fed to the analog digital converter (ADC) channels for the sampling process. After the output voltage (V_{Load}) of the proposed inverter is sensed, then it transformed to the rms form to simplify the controller calculation. Furthermore, a cascaded mode of ADC sequencer function is applied to control the results (AdcRegs.ADCMAXCONV.all). The sinewave voltage which is generated using the function generator and the measured feedback voltage are saved in the ADC input channels (ADCCHSELSEQ1.bit.CONV00) and (ADCCHSELSEQ1.bit.CONV01) respectively. When the ADC conversion is completed, the converted values are stored in its respective registers (ADCRESULT0, ADCRESULT1). However, the error e between the reference voltage ($V_{ref\ rms}$) and the measured ($V_{Load\ rms}$) is computed as shown in equation (10) and then fed to the proposed intelligent controller at every sampling time to generate the $V_{control}$ value which controls the output voltage in order to get a good transient response.

$$\mathbf{e} = \mathrm{V_{ref\,rms}} - \mathrm{V_{Load\ rms}} \tag{10}$$

The digital equation of the proposed PI intelligent controller can be derived from the analog controller equation shown in equation (5) as follows;

$$\mathrm{V_{control}}(z) = \mathrm{k_p}\ \mathrm{e}(z) + \frac{\mathrm{k_i}}{1-z^{-1}}\ \mathrm{e}(z) \tag{11}$$

This derivation can be applied to regulate the inverter output voltage by reducing the steady-state error in order to keep the voltage error $e(z)$ at minimum value. Meanwhile, the overall system is capable to keep the output voltage very close to the reference voltage by using the SPWM power control. On the other hand, the inverter output ($V_{control}$) shown in equation (12) which represents the modulated signal (50 Hz) is compared with the voltage carrier signal ($V_{carrier}$) to generate the IGBTs switching signals. The duty ratio relationship of this comparison is called modulation index or period interrupt (TxPINT) which can be represented as [44];

$$\mathrm{M\ (Modulation\ index)} = \frac{\mathrm{Amplitude\ of\ V_{control}}}{\mathrm{Amplitude\ of\ V_{carrier}}} \tag{12}$$

The ($V_{control}$) amplitude is controlled by the M value, the better range of M is between (0-1). Any value more than 1, it is called over modulation which can be produced more harmonics in the output waveform. The carrier frequency $f_{spwm} = 10KHz$ is chosen for the sine pulse width modulation (SPWM) which depends on the timer period (TBPRD). So, a symmetric carrier frequency signal is applied as shown in equation (13) to obtain a sinusoidal output voltage and decreases its harmonic distortion. Generally, the duration period (positive or negative) of the SPWM output pulses can be generated based on a mechanism comparison between the compare register (TxCMPR, modulated signal which is generated by using function generator) and the timer period (TBPRD) of the SPWM (saw-tooth signal, carrier signal). The timer period (TBPRD) is calibrated in a continuous mode (up/down). When the value stored in the compare register is matched with the timer period value, a positive transition in the digital SPWM output is occurred. Otherwise, a negative transition in the SPWM output is occurred when the second match between the stored values is made again or the clock of timer period is reached to the end in order to return it back to the original status as shown in fig. 4. This action is periodically repeated at every SPWM period for obtaining a new comparison value to change the width of the SPWM output pulses which controls and derives the IGBTs switches signals (S_1,S_2). For more explanation, the code of the proposed control algorithm is presented so far in fig. 5 which is experimentally implemented and tested on the designed prototype inverter illustrated in fig. 1.

$$\mathrm{f_{spwm}} = \frac{\mathrm{f_{cpu}}}{2*\mathrm{f_{TBPRD}}*\mathrm{CLKDIV}*\mathrm{HSPCLK}} \tag{13}$$

Where; f_{spwm} is the switching frequency of the carrier signal, f_{cpu} is the reference frequency of DSP system, f_{TBPRD} is the frequency of the SPWM timer period, $CLKDIV$ is the clock period, and $HSPCLK$ is the high speed clock prescaler.

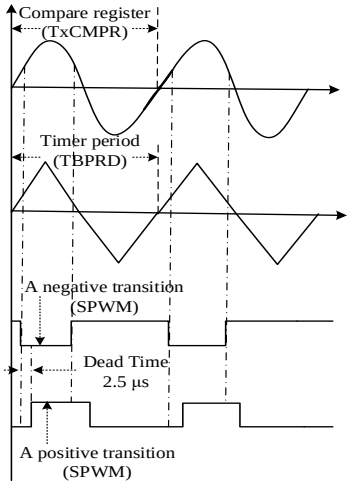

Fig. 4. A Symmetric SPWM generation with timers units

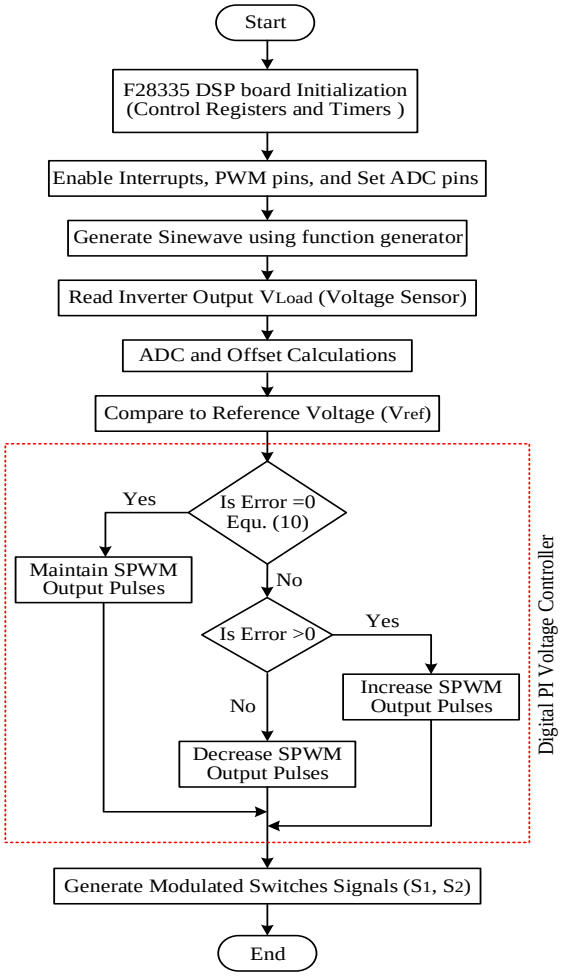

Fig. 5. Proposed Control algorithm flowchart

5. Inverter Experimental Setup

The complete experimental setup of the proposed inverter described in fig. 6 includes; single-phase inverter which designed by using the full-bridge configuration, an LC filter circuit to produce a sinusoidal output voltage, a Laptop with Code Composer Studio (CCS) environment, FLUKE multimeters devices to measure the output of voltage and current, digital storage oscilloscope (Tektronix TDS20204C) to display the waveforms, function generator (INSTEK GPG-8255A) to generate the sinewave voltage waveform, a get driver circuit to connect the F28335 board's output with the IGBTs switches, laboratory DC power supply (INSTEK GPS-3303) to bias the designed get driver circuit, real DC power supply (ISOSEC1) to supply the input voltage, eZdsp F28335 board to implement SPWM control algorithm, voltage and current measurement sensors (LV25-P 716029, LA25-MP 715323), local loads (R_1, R_2, and RL), on/off switch to move between the loads, and differential prope (PINTEK DP-25) to display the real output voltage using oscilloscope. Furthermore, to do the voltage control algorithm of the proposed sine PWM inverter using eZdsp F28335 board, a description of acquisitions circuits are needed to feed the inverter parameters to the proposed controller. For example, the voltage sensor LEM LV25-P (716029) is applied to supply the inverter output voltage to the controller. In addition, RC circuit is used before the eZdsp F28335 board to smooth the sensed voltage and decreases its harmonics. The details of the proposed inverter parameters, voltage sensor, and switches status of SPWM to obtain the AC output voltage across the load are shown in table 1. A F28335 unit board and the Code Composer Studio (CCS) environment have been used to implement the proposed controller and monitor the system performance. Furthermore, a get driver circuit has been used to electrically isolate the control and power circuits through opto-coupler devices.

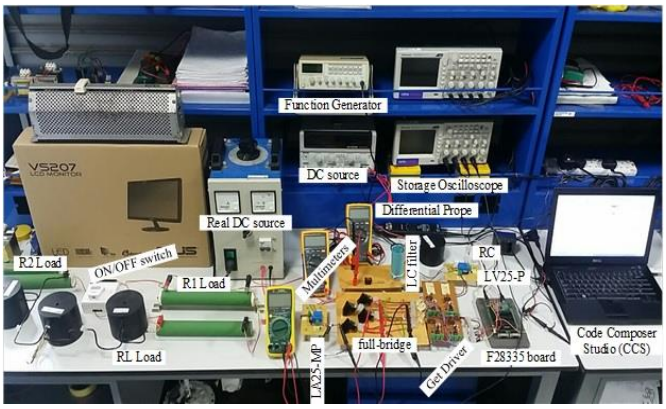

Fig. 6. Experimental setup of proposed inverter

Table 1. Proposed prototype system details

Inverter Parameters	Values
Input DC voltage, V_{dc}	75 V
Filter inductance, L	5 mH SMP made
Filter capacitance, C	15 $\mu F\pm$ 10% , 440 AC, 50 Hz
Resistive loads, R_1 and R_2	(100, 200) Ω, DDR 300W
Inductive load, RL	$100 + j15.7\ \Omega$
Switching frequency, f_s	10 KHz
Fundamental frequency, f	50 Hz
IGBTs (G4PC50UD-326P)	Thresholds; 15 V, 50 mA, 2.5 μs dead time
Voltage Sensor	Details
LV25-P (Voltage Sensor)	0 → 25 mA, 12 → 15 V
Potentiometer (4885293)	500Ω ±25% , 1/5W
LM285LP-1-2 (Shunt Voltage)	1.235V, 1%, 3-Pin TO-92
NMH0515DC(DC-DC	Vin 4.5 →5.5 Vdc, Vout

Converter)	±15Vdc
Switches Status of SPWM	Output Voltage (V_{Load})
S_1 is on and S_2 is off	Positive V_{dc}
S_2 is on and S_1 is off	Negative V_{dc}

6. Results and Discussion

In this section, the simulated model of the proposed inverter shown in figure 1 is implemented to evaluate the effectiveness of the optimum voltage controller using harmony search algorithm based PI (HS-PI). For the optimal system performance, figure 8 displays the convergence characteristics of HS-PI as compared to the convergence characteristics obtained by using PSO algorithm based PI (PSO-PI). In both optimization algorithms, same parameters are used like number of iterations, population size, dimension of problem, and the objective function in equation (7). Based on fig. 7, it is clear that the convergence of the proposed HS-PI is faster than PSO-PI. In other words, the obtained response of the overall inverter system is better and robustness under different loads conditions.

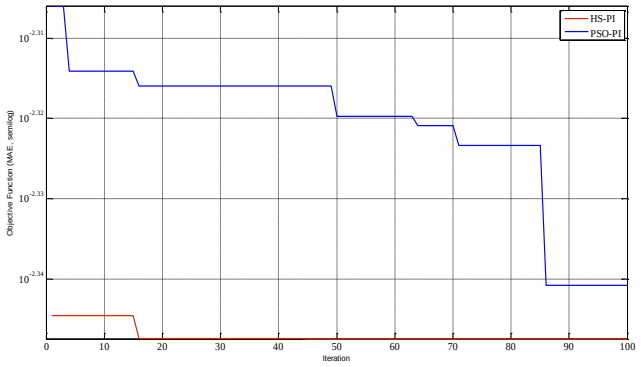

Fig. 7. Objective function performances based on HS-PI and PSO-PI

Furthermore, based on a statistical evaluation, a Wilcoxon test was conducted with P-value equal to 0.05 to verify whether the obtained results by using HS-PI and PSO-PI algorithms are statistically significant. Based on the generated report, the ratio of the p-value for both HS-PI versus PSO-PI is less than 0.05 (p-value <0.05). This is to indicate that the tested iterations which done by HS-PI is statistically better than PSO-PI. In addition, the box plot based on HS-PI and PSO-PI over 50 runs is described in fig. 8 to demonstrate the effectiveness of the obtained solutions distribution by both algorithms. It is shown that the results of solutions distribution which generated by HS-PI is better than PSO-PI and the error value of the objective function (MAE) is 0.00057 for the HS-PI as compared to 0.0016 of PSO-PI.

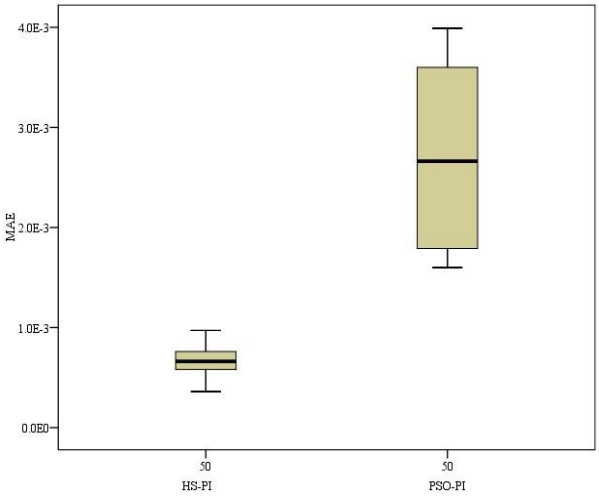

Fig. 8. Box plot of solutions distribution based on HS-PI and PSO-PI

6.1. Resistive Loads (R_1,R_2) Performance

In this case, it has been focused on the output voltage and current waveforms for the overall inverter system based on simulation and experimental hardware results. The experimental hardware results were conducted in this laboratory based on devices and components with low power rated values just to validate the effectiveness and the robustness of the proposed HS-PI inverter controller as compared to the simulation results. The voltage waveform of the experimental setup is measured with differential probe scale is X50 while the current waveform is sent directly to the oscilloscope through a sensor. The simulation results has been carried out for 0.08s and sampling time (Ts) is 1µs with total resistive load is 600W. In fig. 9, the output voltage and current waveforms of the simulation results are validated by the experimental hardware results which are in same phase (unity power factor). This is to indicate that the relationship's efficiency between the voltage and the current is high and both of them are sinusoidal with 50 Hz, resistive load is 100 Ω (R_1), voltage value is approximately 50.72$V\ rms$ (peak value is 50.72*$\sqrt{2}$), and current value is approximately 0.55A rms (peak value is scaled, 0.55*$\sqrt{2}$).

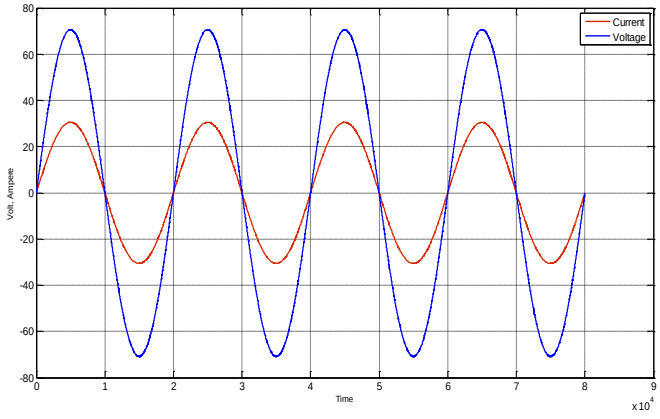

Fig. 9a. Simulation output waveforms with resistive load R_1

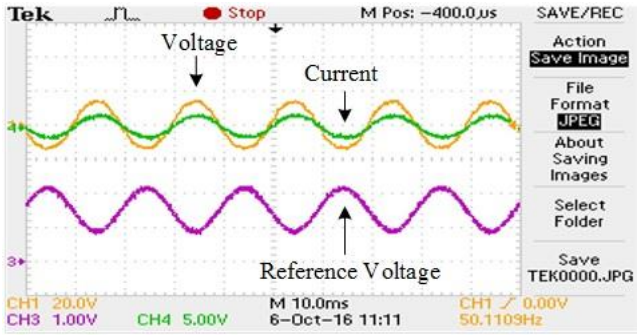

Fig. 9b. Experimental output waveforms with resistive load R_1

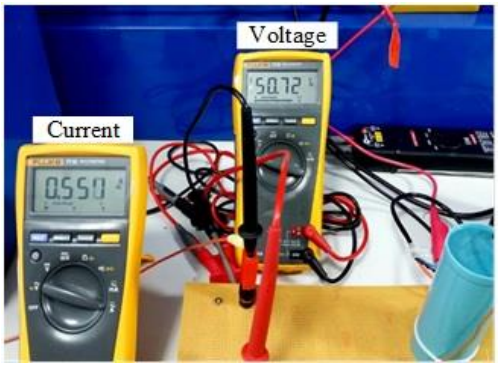

Fig. 9c. Experimental output values in rms with resistive load R_1

For more analysis to see the drop voltage behavior on the inverter output without a controller, another resistive load R_2 (200 Ω) is added to the system. The simulation and experimental output responses of the voltage and current are shown in figs. 10a and b. It is clear that the peak value of the output current in both figures is increased from 0.55*$\sqrt{2}$ to 0.737*$\sqrt{2}$ (peak value is scaled). On the other hand, the voltage and current waveforms are still in the sinusoidal form with unity power factor.

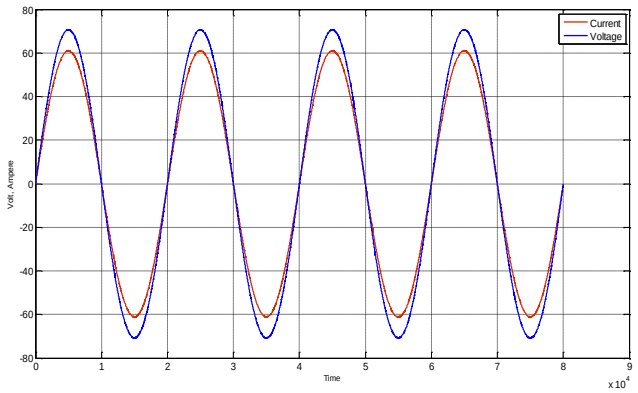

Fig. 10a. Simulation output waveforms with resistive loads (R_1+R_2)

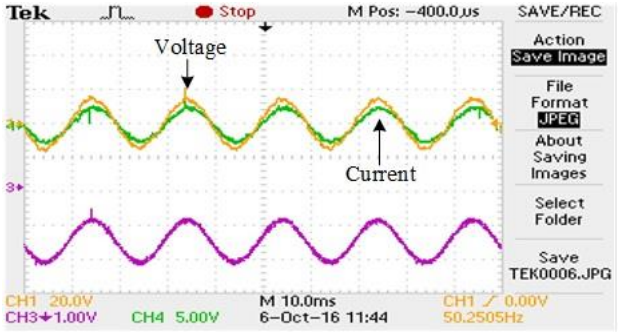

Fig. 10b. Experimental output waveforms with resistive loads (R_1+R_2)

Based on fig. 11a, when R_2 is added to the system, it is clear that the output voltage is dropped from 50.72V rms into 46.63V rms while the output current is increased from o.557A rms to 0.737A rms. To solve this problem, the proposed controller is used as shown in fig. 11b. The voltage value in rms form is fixed at 50.31V while the current value in rms form is 0.782A as compared to fig. 11a. This is to confirm that the proposed controller for regulating the voltage amplitude based on the reference voltage is succeeded under different loads. Meanwhile, the proposed control algorithm for the inverter system is sufficiently robust and stable under different transient operations.

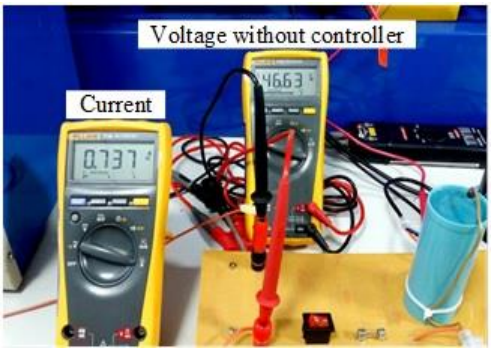

Fig. 11a. Experimental output values in rms with resistive loads (R_1+R_2)

Fig. 11b. Experimental output values in rms with resistive loads (R_1+R_2)

To validate the efficiency and the robustness of the proposed HS-PI controller, a transient operation has been

occurred to the system by step change in R_2 (deceased the load value) through the on/off switch. This changing in the R_2 load will lead to disturb the voltage and current waveforms but the voltage value must be regulated by the proposed controller depending on the error value. When the load is decreased from 600W to 300W (means R_2 is disconnected) at t is equal to $0.04\ s$. Fig. 12a shows the simulation results which are validated by the experimental results as shown in figure12b. Based on decreasing the load, the output voltage will be increased. Therefore, the error will be calculated and then sent to the controller to choose the optimal values of K_p and K_i in order to control and keep the output voltage as close as to the reference voltage at 50Vrms. Furthermore, it is noted that from fig. 12, there is no effect of overshoot or oscillation on the output voltage waveform at the time of $0.04\ s$. This result means that the proposed control algorithm is highly efficient according to the voltage reference.

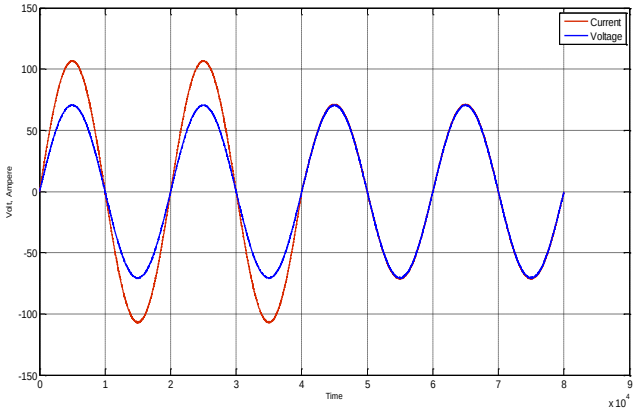

Fig. 12a. Simulation output waveforms with step load change (R_2 disconnected)

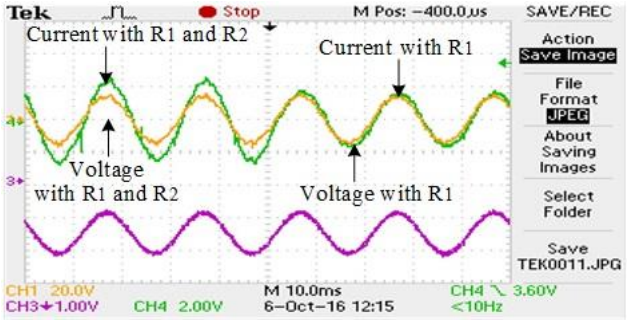

Fig. 12b. Experimental output waveforms with step load change (R_2 disconnected)

6.2. *Resistive Inductive Loads R_L with R_1 performance*

In this case, a second type of load is applied to the system which is called an inductive load (R_L). The main reason of using the R_L load is to test the stability of the proposed controller especially in the output voltage and current waveforms. The equivalent impedance (X_{RL}) of the inductive load is $(100 + j15.7)\ \Omega$ as shown in table 1. Fig. 13 describes the experimental waveforms of the voltage and current with R_L load. It is clear that, there is a phase shift between the voltage and the current across the load. The current waveform lags the voltage waveform by angle is 8.9°. Both of the voltage and current are sinusoidal with 50 Hz, voltage value is 50.72$V\ rms$ (peak value is 50.72*$\sqrt{2}$), and current value 1.007A rms (peak value is scaled, 1.007*$\sqrt{2}$).

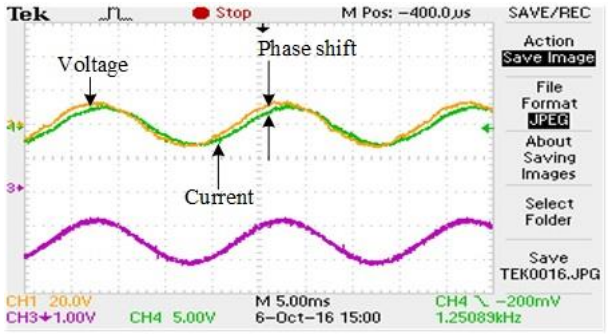

Fig. 13. Experimental output waveforms with R_L load

In fig. 14a, when the load (R_1) is added to the system, there is a voltage drop measured. The voltage value is deceased from 50.72V rms into 45.58V rms while the current value is increased from o.557A rms to 1.007A rms. To overcome this problem, the proposed controller is used as shown in fig. 14b. The voltage value in rms form is fixed at 50.45V while the current value in rms form is 1.007A as compared to figure 14a. This is to demonstrate that the proposed controller for regulating the voltage amplitude based on the reference voltage is succeeded under different loads.

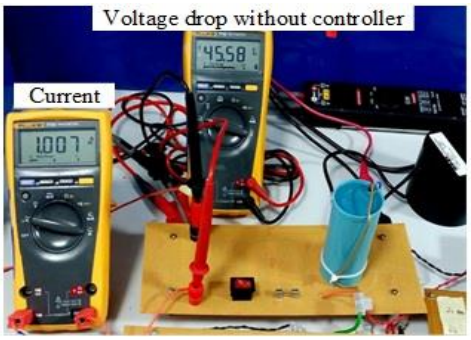

Fig. 14a. Experimental output values in rms with loads (R_1+R_L)

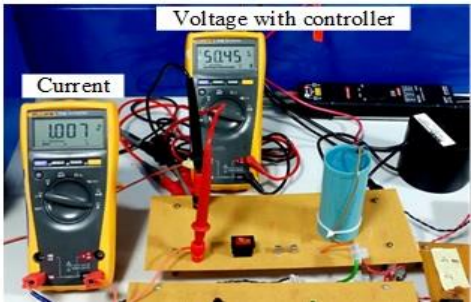

Fig. 14b. Experimental output values in rms with loads (R_1+R_L)

Furthermore, a transient operation has been done for the system to validate the stability of the proposed controller in order to avoid the voltage drop problem shown in figure 14 when the inductive load (R_L) is applied to the system. For the test purpose, the R_1 load is disconnected from the system at t is equal to $0.04\ s$ using the on/off switch. Fig. 15 shows the experimental results of the voltage and currents waveforms. This is to say that the magnitude of the AC output voltage is successfully controlled by the proposed controller which is very close to the reference voltage at 50 Hz. Meanwhile, the output voltage waveform of the inverter remain stable, not affected by the step load change, no steady-state error, and it has good transient performance.

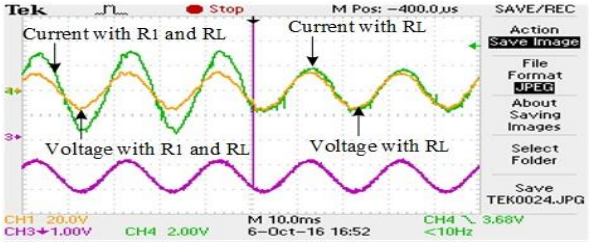

Fig. 15. Experimental output waveforms with step load change (R_1 disconnected)

7. Conclusion

In this research, an optimum digital PI voltage controller has been implemented based on harmony search (HS) algorithm for inverter system with SPWM power control. The implementation of the digital controller linked the inverter hardware has been utilized using the eZdsp TMS320F28335 control unit. The HS algorithm is applied to implement a self-tuning process in getting the PI parameters (k_p,k_i) for the proposed inverter system instead of the trial and error procedure. The mean absolute error (MAE) formula has been used as an objective function to tune the PI parameters by minimizing the voltage error in the inverter output under different loads. As a result, there are tests have been done to demonstrate the system performance. The first test is statistical analysis, a Wilcoxon and box plot tests are done to evaluate the convergence characteristics and the significance of the proposed controller (HS-PI) as compared to the (PSO-PI) controller. It is noted that, the proposed controller is statistically significant, has better performance, and MAE value is 0.000571 of HS-PI as compared to 0.0016 of PSO-PI. The simulation results of the inverter voltage waveform has been validated by the experimental results in the second test to evaluate the effectiveness and the robustness of the proposed controller. Meanwhile, it has provided a very good transient specifications in terms of voltage amplitude and it also has no negative effects or oscillation.

References

[1] G.E. Ahmad, H.M.S. Hussein, H.H. El-Ghetany, "Theoretical analysis and experimental verification of PV modules", *Renewable Energy*, Vol. 28, pp. 1159–1168, 2003.

[2] M.A.A. YOUNIS, Tamer KHATIB, M. A, A Mohd ARIFFIN "An Improved Maximum Power Point Tracking Controller for PV Systems Using Artificial Neural Network "*Journal of Electrical Review*, ISSN 0033-2097, Vol. 88, Issue NR 3b, pp. 116-121, 2012.

[3] A. Chel, G.N. Tiwari, A. Chandra, "Simplified method of sizing and life cycle cost assessment of building integrated photovoltaic system", *Energy and Buildings*, Vol. 41, pp. 1172–1180, 2009.

[4] M. Ali, Mohd Herwan Bin Sulaiman, Mojgan Hojabri, Hussein M. Hamada and Mushtaq N. Ahmed, "A Review *on Photovoltaic Array Behavior, Configuration Strategies and Models under Mismatch Conditions", ARPN Journal of Engineering and Applied Sciences*, Vol. 11, No. 7, pp. 4896-4903, 2016.

[5] N. Mushtaq, Mojgan Hojabri, Hamdan bin Daniyal, Ali M. Humada, "Maximum Power Prediction for PV System based on P&O Algorithm", *Journal of Advanced & Applied Sciences* ,Vol. 3, No. 4, pp.113-118, 2015.

[6] Jayalaksmi N. S., D. N. Gaonkar, Anandh N. and Nimika Sanjeev Kumar, Design and Implementation of Single Phase Inverter Based on Cuk Converter for PV System, *International Journal of Renewable Energy Research*, Vol.7, No.2, 2017.

[7] Manoj B Anurag; Gunda Sai Thrinath; Srinivas Bhaskar Karanki; Ram Yallamili, Design of ZVS based high gain DC-DC converter for PV applications, *IEEE International Conference on Renewable Energy Research and Applications (ICRERA)*, pp. 584 - 589, DOI: 10.1109/ICRERA.2016.7884402, 2016.

[8] Sperati, S.; Alessandrini, S.; Pinson, P.; Kariniotakis, G. "The Weather Intelligence for Renewable Energies Benchmarking Exercise on Short-Term Forecasting of Wind and Solar Power Generation", *Energies*, Vol. 8, No. 9, pp. 9594–9619, 2015.

[9] Mushtaq N., Mojgan Hojabri, A. Humada, Hamdan Bin Daniyal, Hatem Fahad Frayyeh, "An Overview on Microgrid Control Strategies", *International Journal of Engineering and Advanced Technology*, Vol. 4 No. 5, pp. 93-98, June 2015.

[10] M. Ali, Mojgan Hojabri, Mohd Herwan Bin Sulaiman, Hussein M. Hamada, Mushtaq N., "Photovoltaic Grid-Connected Modeling and Characterization Based on Experimental Results", *PLOS ONE*, Vol. 11, No. 4, pp. 1-13, 2016.

[11] F. Blaabjerg, Z. Chen, S. Kjaer, "Power electronics as efficient interface in dispersed power generation systems", *IEEE Transactions on Power Electronics*, Vol. 19, pp. 1184–1194, 2004.

[12] Ali Mahmood, Mojgan Hojabri, M. Najeeb, "Reconfiguration Method Based on DC-DC Central Converter within Different Mismatch Conditions", *International Journal of Engineering Sceince & Reseach Technology*, Vol. 2, No. 12, pp. 3634-3639, 2013.

[13] M.N. Amrani, A. Dib, Predictive Direct Power Control of a Grid Connected Three-Phase Voltage Source Inverter for Photovoltaic Systems, *International Journal of Renewable Energy Research*, Vol.6, No.1, 2016.

[14] Kivanc Basaran; Numan Sabit Cetin, Designing of a fuzzy controller for grid connected photovoltaic system's converter and comparing with PI controller, *IEEE International Conference on Renewable Energy Research and Applications (ICRERA)*, pp. 102 - 106, DOI: 10.1109/ICRERA.2016.7884437, 2016.

[15] Youcef Soufi; Mohcene Bechouat; Sami Kahla; Kais Bouallegue, Maximum power point tracking using fuzzy logic control for photovoltaic system, *International Conference on Renewable Energy Research and Application (ICRERA)*, pp. 902 - 906, DOI: 10.1109/ICRERA.2014.7016515, 2014.

[16] Ortega, R.; Figueres, E.; Garcerá, G.; Trujillo, C.L.; Velasco, D. "Control techniques for reduction of the total harmonic distortion in voltage applied to a single-phase inverter with nonlinear loads: Review", *Renewable and Sustainable Energy Reviews*, Vol. 16, No. 3, pp. 1754–1761, 2012.

[17] Selvaraj, J.; Rahim, N.A. "Multilevel Inverter for Grid-Connected PV System Employing Digital PI Controller", *IEEE Transactions on Industrial Electronics*, Vol. 56, No. 1, pp. 149–158, 2009.

[18] B.Krishna Naick, T.K.Chatterjee, K.Chatterjee, Fuzzy Logic Controller based PV System Connected in Standalone and Grid Connected Mode of Operation with Variation of Load, *International Journal of Renewable Energy Research*, Vol.7, No.1, 2017.

[19] Sanchis, P.; Ursaea, A.; Gubia, E.; Marroyo, L. "Boost DC-AC Inverter: A New Control Strategy", *IEEE Transactions on Power Electronics*, Vol. 20, No. 2, pp. 343–353, 2005.

[20] A. Muthuramalingam, S.V. Vedula, P.A. Janakiraman, "Performance evaluation of an FPGA controlled soft switched inverter", *IEEE Transactions on Power Electronics*, Vol. 21, pp. 923–932, 2006.

[21] M. Sreedevi, P.J. Paul, "Fuzzy PI controller based grid-connected PV system", *International Journal of Soft Computing*, Vol. 6, pp. 11–15, 2006.

[22] Ghani, Z.A.; Hannan, M.A.; Mohamed, A. "Simulation model linked PV inverter implementation utilizing dSPACE DS1104 controller", *Energy and Buildings*, Vol. 57, pp. 65–73, 2013.

[23] A. Hmidet, R. Dhifaoui, O. Hasnaoui, "Development, implementation and experimentation on a dSPACE DS1104 of a direct voltage control scheme", *Journal of Power Electronics*, Vol. 10, pp. 468–476, 2010.

[24] M.A. Hannan, Z.A. Ghani and A. Mohamed, "An Enhanced Inverter Controller for PV Applications Using the dSPACE Platform", *International Journal of Photoenergy*, vol. 2010, doi:10.1155/2010/457562, pp 1-10, 2010.

[25] Daud, M.Z.; Mohamed, A.; Hannan, M.A. "An Optimal Control Strategy for DC Bus Voltage Regulation in Photovoltaic System with Battery Energy Storage", *Scientific World Journal*, Vol. 2014, pp. 1-16, 2014.

[26] Liserre, M.; Dell'Aquila, A.; Blaabjerg, F. "Genetic Algorithm-Based Design of the Active Damping for an LCL-Filter Three-Phase Active Rectifier", *IEEE Transactions on Power Electronics*, Vol. 19, No. 1, pp. 76–86, 2004.

[27] Li, W.; Man, Y.; Li, G. "Optimal parameter design of input filters for general purpose inverter based on genetic algorithm", *Applied Mathematics and Computation*, Vol. 205, No. 2, pp. 697–705, 2008.

[28] Sundareswaran, K.; Jayant, K.; Shanavas, T.N. "Inverter Harmonic Elimination through a Colony of Continuously Exploring Ants", *IEEE Transactions on Industrial Electronics*, Vol. 54, No. 5, pp. 2558–2565, 2007.

[29] Mohamed, Y.A.I.; El Saadany, E.F. "Hybrid Variable-Structure Control with Evolutionary Optimum-Tuning Algorithm for Fast Grid-Voltage Regulation Using Inverter-Based Distributed Generation", *IEEE Transactions on Power Electronics*, Vol. 23, No. 3, pp. 1334–1341, 2008.

[30] Yoshiki Ikai; Nobukazu Hoshi, Expanding ZVS range for dual active bridge DC-DC converter using three-level neutral-point-clamped inverter topology, *IEEE International Conference on Renewable Energy Research and Applications (ICRERA)*, pp. 472 - 477, DOI: 10.1109/ICRERA.2016.7884382, 2016.

[31] Valentin Oleschuk; Vladimir Ermuratskii; Frede Blaabjerg, Six-phase vehicular drive with renewable dc sources and hybrid PWM control of four inverters, International Conference on Renewable Energy Research and Applications (ICRERA), pp. 515 - 519, DOI: 10.1109/ICRERA.2015.7418466, 2015.

[32]Noradin Ghadimi, "PI Controller Design for Photovoltaic Systems in Islanding Mode Operation", *World Applied Sciences Journal*, Vol. 15, No. 3, pp. 326-330, 2011.

[33] Mohan, N.; Undeland, T.M.; Robbins, W.P. "Power Electronics: Converters, Applications, and Design", 3rd ed.; *John Wiley and Sons*: Hoboken, NJ, USA, 2003.

[34] Mohammad Monfared, Saeed Golestan, and Josep M. Guerrero, "Analysis, Design, and Experimental Verification of a Synchronous Reference Frame Voltage Control for Single-Phase Inverters", *IEEE Transactions on Industrial Electronics*, Vol. 61, No. 1, 2014.

[35] Mushtaq N. Ahmed, Mojgan Hojabri, Hamdan bin Daniyal, Ali Mahmood Humada, " Simulation of Regulated Power Supply for Solar Photo-Voltaic Model", *International Journal of Engineering Sceince & Reseach Technology*, Vol. 2, No. 12, pp. 3607-3613, Dec. 2013.

[36] Sasmita Behera, Bidyadhar Subudhi, Bibhuti Bhusan Pati, "Design of PI Controller in Pitch Control of Wind Turbine: A Comparison of PSO and PS Algorithm", *International Journal of Renewable Energy Research*, Vol.6, No.1, pp. 271-281, 2016.

[37] M. N., Mohammed Shahooth, Arrak Mohaisen, Ramdan bin Razali and Hamdan bin Daniyal, "An optimized PID parameters for LFC in interconnected power systems using MLSL optimization algorithm", ARPN Journal of Engineering and Applied Sciences, Vol. 11, No. 19, pp. 11770-11781 Oct. 2016.

[38] D. Manjarres, I. Landa-Torres, S. Gil-Lopez, J. Del Ser, M.N. Bilbao, S. Salcedo-Sanz, Z.W. Geem, "A survey on applications of the harmony search algorithm", *Engineering Applications of Artificial Intelligence*, Vol. 26, No. 8, pp. 1818–1831, 2013.

[39] Esam Taha Yassen, Masri Ayob, Mohd Zakree Ahmad Nazri, and Zulkifli Ahmad, "Harmony Search Algorithm for Vehicle Routing Problem with Time Windows'", *Journal of Applied Sciences*, Vo. 13, No. 4, pp. 633-638, 2013.

[40] Das, S., A. Mukhopadhyay, A Roy, A Abraham and B.K. Panigrahi, "Exploratory power of the harmony search algorithm: Analysis and improvements for global numerical optimization", *IEEE Transactions on Systems*, Vol. 41, No. 1, pp. 89-106, 2011.

[41] Liu, L. & H. Zhou, "Hybridization of harmony search with variable neighborhood search for restrictive single-machine earliness/tardiness problem", *Information Sciences: an International Journal*, Vol. 226, pp. 68-92, 2013.

[42] Ammar Hussein Mutlag, Azah Mohamed, and Hussain Shareef, "A Nature-Inspired Optimization-Based Optimum Fuzzy Logic Photovoltaic Inverter Controller Utilizing an eZdsp F28335 Board", *Energies*, Vol. 9, No. 120, pp. 1-32, 2016.

[43] Jamal Abd Ali, M A Hannan, Azah Mohamed, Maher G.M. Abdolrasol, "Fuzzy logic speed controller optimization approach for induction motor drive using backtracking search algorithm", *Measurement*, Vol. 78, pp. 49–62, 2016.

[44] V. M. Deshmukh1, A. J. Patil, P. V. Thakre, "Development of Matlab/Simulink Model for Three Phase PWM Inverter and Hardware Implementation and Testing Using DSP with Nonlinear Load", *International Journal of Control Science and Engineering*, Vol 5, No. 1, pp. 1-9, 2015.